

An Experimental and Numerical Study of Tire/Pavement Noise on Porous and Nonporous Pavements

L. M. Dai^{1,2,*} and Z. Lou^{1,2}

¹*Mathematics and Physics, North China Electric Power University, Beijing 102206, P. R. China*

²*Industrial Systems Engineering, University of Regina, Regina, Saskatchewan S4S 0A2, Canada*

Received 12 April 2007; revised 18 October 2007; accepted 27 December 2007; published online 30 May 2008

ABSTRACT. This present research assesses tire/pavement noise by analyzing and comparing noise data acquired from low noise pavement (Asphalt Rubber Concrete) and conventional pavement (Asphalt Concrete). Close Proximity (CPX) tests are employed in this research to acquire the tire/pavement noise generated from the test pavements. A numerical simulation model established via the finite element method is conducted to simulate the noise generated by the impact mechanism, which is observed from the CPX test on both the test pavements. The simulated tire/pavement noise pressure levels are compared with those tested to verify the reliability of the numerical model.

Keywords: tire/pavement noise, traffic noise reduction, CPX tests, ARC, AC, numerical simulation in acoustics

1. Introduction

Noise may induce many negative effects in human beings, physiologically and psychologically. With many technologies developed to reduce industrial noise, traffic noise has become a major noise resource disturbing the normal lives of people in urban areas. Nowadays, environmental pollution caused by traffic noise is very serious in urban areas. The general acceptable traffic noise level for residential areas should be less than 55 dBA (WHO, 1999). In many big cities, traffic noise levels of some streets can reach more than 80 dBA (Li et al., 2002; Ali and Tamura, 2003). This high noise pressure level is harmful to human health. Thus, decent activities for traffic noise reduction need to be implemented in areas where the traffic noise is so high that residents are seriously disturbed.

Tire/pavement sourced noise has been proven to be the major sources of traffic noise for cruise driving conditions, especially for light vehicles (Sandberg and Ejsmont, 2002), which is the dominant form of traffic in urban areas. de Graaff and van Blokland (1997) indicated that about 90% of the equivalent sound energy in urban traffic is generated by tire/pavement noise. Thus, reducing tire/pavement noise can be an efficient method for traffic noise control, especially for urban traffic noise control. Porous pavement has been proven to have a higher ability to reduce traffic noise, especially tire/pavement

sourced noise (Meiarashi et al., 1996). According to the studies conducted, the noise reducing principles of porous pavements can be concluded as follows:

Absorption of aerodynamic sourced energy. Aerodynamically generated sound energy is created by air displaced into/out of cavities in or between tire treads and pavement surfaces while the tire is in contact with the pavement surface (Sandberg and Ejsmont, 2002). The open texture creates a porosity that prevents the creation of high air pressure gradients at the edges of the tire/road contact patch and within the contact patch. As a result, the sound created by air pumping could be reduced because of aerodynamic power reduction.

Sound absorption. Sound waves carry a certain amount of energy, called sound energy. When a sound wave hits a material, a portion of the sound energy will be reflected or "bounced" back. The less sound being reflected, the better the acoustic performance of the pavement surface. The porosity in the porous structure creates a sound absorption effect so the sound wave is dissipated into heat within the narrow pores of the pavement.

Changing sound reflection geometry. The traffic noise heard by people consists of two parts — one is the sound wave generated from the noise sources, which include mechanical sourced noise (engine and electric fan noise) and the noise generated directly from the interaction between the tire and pavement. The other part is the noise reflected by the pavement surface. The surface of porous pavement is much rougher than that of nonporous pavement because of the voids on the pavement surface. Thus, the surface of porous pavement can be considered an unreflective surface compared with that of nonporous pavement. The reflected sound power is dispers-

* Corresponding author. Tel.: +1 306 5854498; fax: +1 306 5854855.
E-mail address: dailiml@126.com (L. M. Dai).

ed by the voids' surfaces. Therefore, to the receiver, sound power reflected by porous surfaces is much lower than that of reflective surfaces.

In the present research, tire/pavement noise is studied by analyzing and comparing the noise data from the porous pavement and the nonporous pavement with utilizing a Close Proximity (CPX) test. The CPX test is designed specifically for testing the tire/pavement noise on the roads considered by this research. In the tests, the microphones are located close to the tire/pavement interaction so the effect of noise emitted by other noise resources, such as engine and exhaust noise, can be diminished. The test standard available for the CPX test is ISO/CD 11819-2 (IOS, 1997).

The porous pavement studied in this research is Asphalt Rubber Concrete (ARC) and the nonporous pavement is Asphalt Concrete (AC). The CPX test was conducted on the ARC test section of Saskatchewan. The test section is located on Highway 11 and it was constructed by the Department of Saskatchewan Highways and Transportation. The test section consists of four lanes — two lanes in each direction. The driving lanes in each direction are paved with ARC and the passing lanes are paved with AC. The tire/pavement noise data for porous pavement are acquired from the driving lanes and that of nonporous pavement are acquired from the passing lanes.

Mathematical and numerical noise prediction models are also very useful for tire/pavement studies. They can be employed to optimize the design of tire or pavement to acquire better acoustic performance and they can also benefit the researchers to create a better understanding of the noise generation mechanism. However, the simulation of tire/pavement is a great challenge to traffic noise studies because of the complexity of the noise generation mechanism. It is a multi-physics problem that concerns the topics of structure statistics/dynamics and fluid dynamics. The finite element method (FEM) has proven to be effective in solving this sort of problem. In this research, a world-leading FE software ANSYS (a commercial FE software designed by ANSYS, Inc. Corporate, which was founded in 1970) is employed to acoustically analyze one of the important tire/noise generation mechanisms — tread impact, which is observed from the field tests.

2. CPX Test Design

2.1. Test Microphone Positions

In reference ISO/CD 11819-2, there are six microphone positions selected in the test to present the sound level distribution close to the tire/pavement interface. The microphone positions can be classified into three groups according to the distance between the microphones and the tire surface — inner, middle and outer. Each microphone group includes two positions — front and rear. The layout for the microphone positions is shown in Figure 1. The detailed geometric dimensions for the arrangement of the microphones are tabulated in Table 1.

2.2. Test Trailer Design

For the CPX test, a single-axle trailer is designed, fabric-

cated and used as the vehicle for road tests. Figure 2 shows the CPX test trailer used in the filed tests. The microphones are mounted close to one tire of the trailer. The microphone mount structure is jointly designed by the University of Regina Acoustics Research Group and the Saskatchewan Highways and Transportation Department, Saskatchewan, Canada. The mounting arrangement and the structure of the microphones are shown in Figure 3.

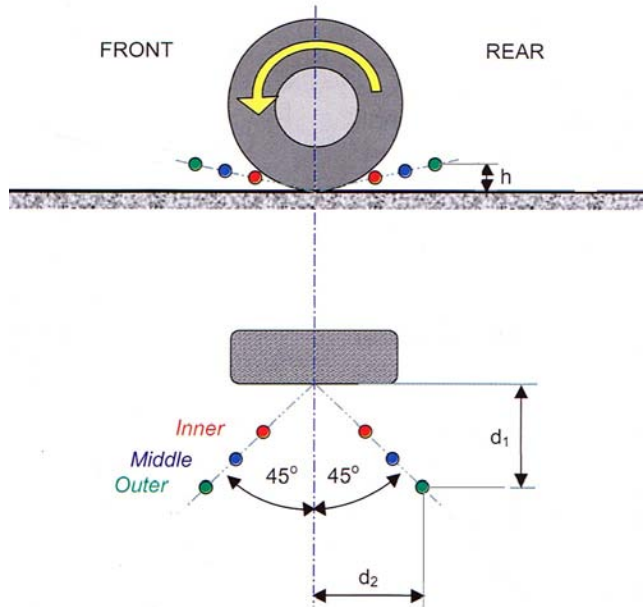


Figure 1. The CPX test microphone positions.



Figure 2. CPX test trailer.

Table 1. CPX Test Microphone Positions

Microphone	h	d_1	d_2	$d_3 = d_1\sqrt{2}$
1. Inner	100 mm	200 mm	200 mm	283 mm
2. Middle	150 mm	300 mm	300 mm	424 mm
3. Outer	200 mm	400 mm	400 mm	566 mm

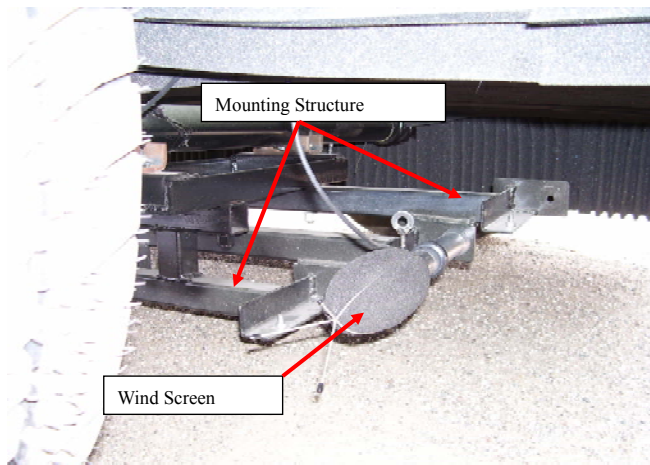


Figure 3. Microphone mounting structure and wind screen.

Since the CPX test is conducted on a moving vehicle, the aerodynamic noise becomes a major contributor that may affect the accuracy of the tire/pavement noise level. The aerodynamic noise includes the noise of wind turbulence generated by the airflow around the microphones while it is moving and external turbulence caused by towing the vehicle. During the test trailer design, three treatments are employed to decrease the influence of aerodynamic noise in the test.

The first treatment involves mounting the microphone support on the inside of the trailer body instead of the common method — mounting the microphone on the outer side of the trailer so that the trailer body can be utilized as a screen. The speed of airflow inside the trailer body is lower than outside the trailer body. As a result, wind turbulence around the microphone can be reduced. This design is based upon the assumption that the dynamic tire conditions on the inner and outer sides of the trailer are the same while the tire is rotating. However, for this design, the noise produced by the other tire would affect the test result. Therefore, an obstacle between the two tires is needed to block noise from the other tire. On the other hand, because the tests are conducted on the highway with free traffic conditions, the design — mounting the microphone inside the trailer body, can reduce the width of the test trailer so the impact of the test on traffic flow can be reduced.

The second treatment is an enclosure around the test tire. The enclosure can reduce the vehicle's aerodynamic airflow. Moreover, the enclosure and the trailer body constitute a screen for blocking the noise generated from other noise sources.

The third treatment employs the 150 mm microphone wind screen to cover the test microphone, which decreases the wind turbulence inside the trailer enclosure. However, the trailer body and enclosure create a housing that can reflect the noise coming from the tire/road interaction. To decrease the reflected noise, the sound absorption material — Z-Foam 12" Panel, which is produced by the Primacoustic company, is attached to the inner surface of the trailer body and enclosure.

The tire pattern can influence tire/road noise. Based on the information provided by the tire dealers in the Regina region,

the universal tire is the most commonly used tire adopted for light automobiles in this region. In order to let our test fit real conditions, the universal tire LXR (P225/60 97T) was selected as the test tire.

2.3. Test Speed and Segment

The test speeds for the CPX test were 50 km/h, 80 km/h and 110 km/h. The three speeds represent the average vehicle speeds on city roads of residential areas, high-speed city roads and highways, respectively.

According to ISO/CD 11819-2, for each test speed, the test road segment should be no less than 20 m. To satisfy this requirement, during the test, the speed of the test vehicle is kept constant for about 20 seconds at each reference speed for data acquisition. Then 10 s of continuous data are acquired as a data group for analysis. Thus, the test distance for the lowest test speed, 50 km/h, is about 138 m which fulfills the required distance. In order to decrease the error caused by uncertain factors, six groups of data are recorded for each microphone position and speed. The test segment is chosen randomly along the test road section. Then the tire/pavement noise pressure levels for a given speed and microphone position can be averaged.

3. CPX Test Process

The CPX tests used to compare the acoustic performance of ARC and AC pavements were conducted in August and September, 2006. The tests were performed under weather conditions with no rain and little wind. The air temperature was about 15 to 30 degrees during the test. The tests are performed on the open highway, to avoid the influence of noise and vibration generated from other vehicles, the noise pressure levels were recorded when there were no vehicles near the test trailer. During the test the B&K 4489 microphone is mounted on the test trailer. The sound level is recorded with a B&K sound intensity meter 2260. The sound is collected in the form of a 1/3-octave band. The equivalent sound-weighting network is A-weighted. The sound recording period is set at 1 second, which means the sound data is recorded every second.

4. Analysis of CPX Test Results

4.1. A-Weighted Equivalent Noise Pressure Levels

Table 2 shows the A-weighted noise pressure levels for each microphone position and speed and their standard deviations. Figure 4 shows the comparison of noise pressure levels under a variety of microphone positions with different vehicle speeds. The standard deviations of all the A-weighted noise pressure levels are lower than 1 dBA. Thus, the noise levels with the same test parameters are the same on either the ARC or AC pavements. This proves the acoustic performance of each test section is uniform for either ARC or AC pavement. The low standard deviation values also prove the credibility of the recorded tire/pavement noise data.

For most microphone positions and speeds, the noise pre-

Table 2. A-weighted Noise Pressure Levels for Each Microphone Position and Vehicle Speed

Speed (km/h)	Microphone position		ARC L_{Aeq} (dBA)	Standard Deviation	Conv. L_{Aeq} (dBA)	Standard Deviation	Difference ARC-Conv. (dBA)
50	Front	Outer	86.78	0.48	85.72	0.48	1.06
		Middle	87.73	0.67	87.31	0.68	0.42
		Inner	90.00	0.62	89.12	0.42	0.88
	Rear	Outer	84.68	0.42	86.01	0.49	-1.33
		Middle	85.31	0.64	88.08	0.74	-2.77
		Inner	88.03	0.73	89.28	0.43	-1.25
80	Front	Outer	92.80	0.57	93.39	0.49	-0.59
		Middle	94.11	0.47	94.80	0.46	-0.69
		Inner	96.54	0.51	96.88	0.64	-0.34
	Rear	Outer	90.39	0.51	93.31	0.49	-2.92
		Middle	91.89	0.49	95.21	0.52	-3.32
		Inner	93.98	0.44	96.69	0.68	-2.71
110	Front	Outer	98.25	0.49	98.89	0.37	-0.64
		Middle	99.28	0.57	99.73	0.3	-0.45
		Inner	101.74	0.48	102.16	0.37	-0.42
	Rear	Outer	94.98	0.39	98.03	0.28	-3.05
		Middle	96.62	0.42	99.37	0.34	-2.75
		Inner	98.08	0.34	101.15	0.46	-3.07

ssure levels tested over the ARC pavement are lower than those tested from AC pavement except for the front microphone at 50 km/h. This indicates ARC pavement has the ability to reduce tire/pavement noise. However, from Table 2, the noise pressure level reductions for the front microphone positions on the ARC are not as significant as those of the rear microphone positions. In most cases, the difference in noise pressure levels between ARC and AC pavement are less than 1 dBA for the front microphone positions. The great noise reductions from ARC pavement are demonstrated by the rear microphone position data. The range in noise reduction for all the rear microphone positions and speeds is 1 dBA to 3 dBA, which is higher than those of the front microphone positions. The magnitude of the noise pressure level reduction increases with increasing vehicle speed. The reduction range increases from 1 to 2 dBA at 50 km/h to approximately 3 dBA at the speed of 80 and 110 km/h. This phenomenon indicates that ARC pavement has better tire/pavement noise reduction ability at high speeds of the vehicle used.

The major sources of tire/road noise are located near the leading and trailing edges of the tire/road contact patch (Sandberg and Ejsmont, 2002). Structure-born vibration and aerodynamic mechanisms are the two major mechanisms for noise originating from the tire/pavement contact patch. For the leading edge, both the mechanism of structure-born vibration and the aerodynamic mechanism play important roles in noise generation. However, the aerodynamic mechanism provides a greater contribution to the noise generated from the trailing edge than the structure-born vibration. Since ARC is porous pavement, there are many voids on the pavement surface and inside the pavement. These create spaces to reduce the streng-

th of the air pumping, which is a major aerodynamic mechanism for tire/pavement noise generation, by preventing air compression. As a result, the noise reduction of the trailing edges is higher than those at the leading edge on ARC pavement.

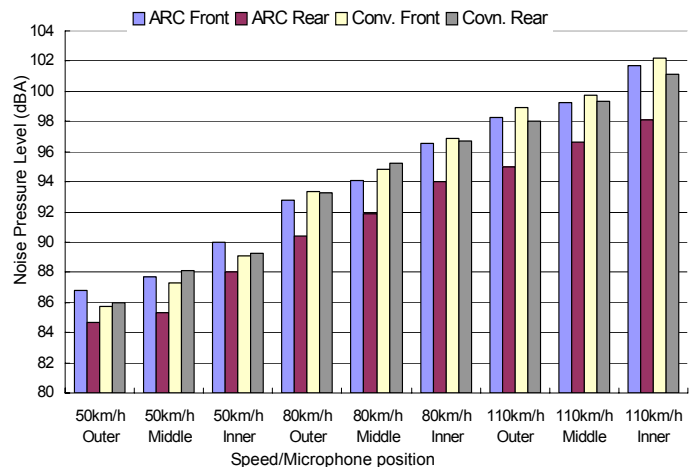


Figure 4. Comparison of noise pressure levels under a variety of microphone positions with different vehicle speeds.

4.2. Spectrum Noise Level Analysis of CPX Test

4.2.1. Comparison of Spectra Noise Pressure Levels on ARC and AC Pavement

The inner microphone positions for the CPX test are recommended by the ISO/CD 11819-2 standard. As a result, the noise pressure levels acquired by the inner microphones are

employed to compare the spectral acoustic performance on the ARC and AC pavements.

Figures 5 and 6 show the spectral noise levels from the front and rear microphone positions, respectively. In this analysis, the data at 50 and 110 km/h were selected to represent the noise pressure levels at low and high speeds. In these two figures, all the spectral noise level curves on the different pavements and at different speeds have a similar trend. The noise pressure levels at low frequencies are higher than those at high frequencies in the frequency range between 800 Hz and 1000 Hz where a noise pressure peak appears. The noise pressure in this range is much higher than in adjacent frequencies.

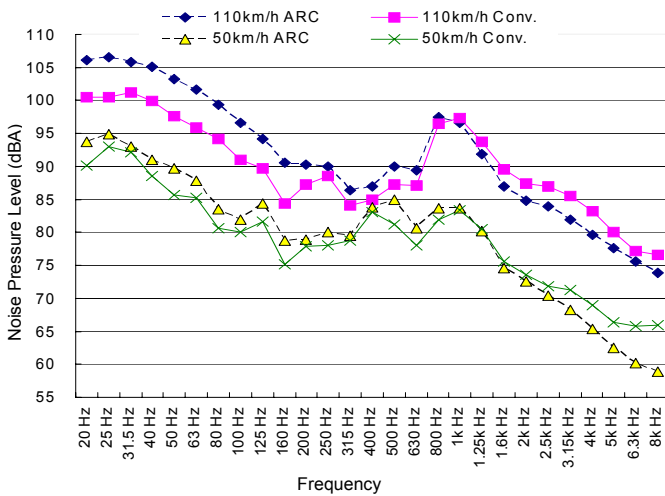


Figure 5. Spectra noise levels of front microphone position.

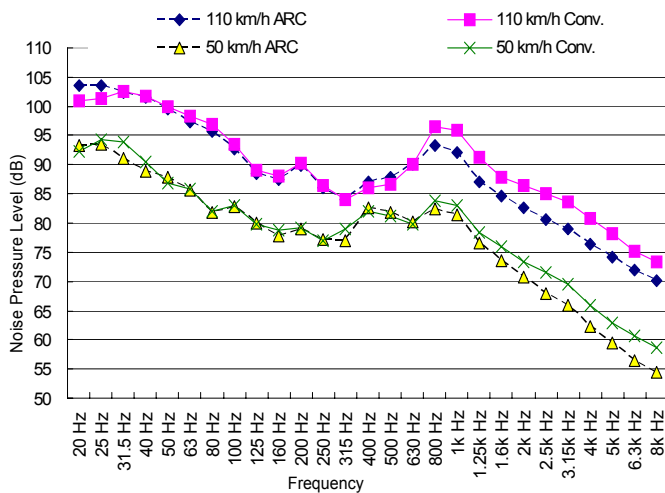


Figure 6. Spectra noise levels of rear microphone position.

The noise reduction on the ARC pavement can be found in the frequency range higher than 1 kHz for both the front and rear microphone positions. However, there is a significant difference between the noise level curves of the front and rear

microphone positions. At the front microphone position, the low frequency noise levels (less than 315 Hz) on the ARC pavement are much higher than those on AC pavement. Comparatively, for the rear microphone position, the noise levels over the two pavements in the same frequency range are not as different as those for the front microphone positions. The same phenomenon can also be found in the spectral noise results acquired from field tests. In the low frequency range, noise pressure levels of the ARC pavement are higher than those in the high frequency range and the obvious noise reduction of the ARC pavement is shown only in the high frequency range.

In A-weighted networks, the weights given to noise pressure levels at high frequencies are higher than those in the low frequency range. Therefore, the results of the A-weighted equivalent noise pressure level and the noise pressure level spectrum can be related for the following reasons. The tested A-weighted equivalent noise pressure levels of the front microphone positions on both pavements are not significantly different because the noise reduction in the high frequency range can counteract high noise levels in the low frequency range. Great noise reduction appears at the rear microphone positions because the reduction in noise pressure levels is present in the high frequency range. This phenomenon proves that ARC pavement is more efficient in reducing tire/pavement noise pressure levels in the high frequency range.

4.2.2. The Impact of Speed on the Noise Pressure Level Spectrum

The noise pressure levels are magnified with increasing speed on both spectral curves in Figures 7 and 8 in the frequency ranges under 100 Hz and higher than 1k Hz. The linear relationship between noise pressure levels and speed can be found in these figures. This means the noise energy generated by certain mechanisms corresponding to certain noise frequency ranges increase as the speed increases. However, the frequency of the noise generated by such mechanisms is not influenced by the speed. However, an irregular range can be found between 125 Hz and 1 kHz. In this range, the linear relationship between noise pressure levels and speed does not exist. Some irregular high noise pressure levels appear on the spectral noise level curves. These noise pressure levels are marked in Figures 7 and 8. The frequencies of these irregular high noise pressure levels correspond to noise frequencies generated by the impact mechanism.

The impact mechanism of a tire occurs on the treading edge of the tire/pavement contact patch during tire rotation. The tread blocks of the treading edge hit the texture of the pavement surface. The force generated by the impact causes the sudden displacement of the tread blocks and pushes the tread block in toward the tire's rotational center. Thus, the sound generated by the deflection and vibration of the tire tread blocks causes the impact mechanism.

The tire surface is not smooth. There are blocks on the tire surface, which are designed for increasing the friction between the tire and surface. The force caused by the impact is

not continuous. It is only in effect while the tread block of the treading edge is in contact with the pavement surface. The force disappears during the gaps between the tread blocks rotating on the contact patch. For most tires available on the commercial market, the tire tread block is arranged regularly. The tire's rotational speed is kept constant while the vehicle drives at a constant speed. Thus, the regularly arranged tread blocks hit the pavement surface at a constant rhythm. This phenomenon is the same as a hammer hitting the tire surface at a certain frequency. According to research by Larsson (2002), the frequency of the impact force is dependent upon the distance between the tread blocks and the speed of the vehicle. The frequency of the impact force can be described by the following equation:

$$f_s = v / \lambda \tag{1}$$

where f_s is the frequency of impact force in Hz, v is the vehicle speed in m/s and λ is the distance between tire tread blocks.

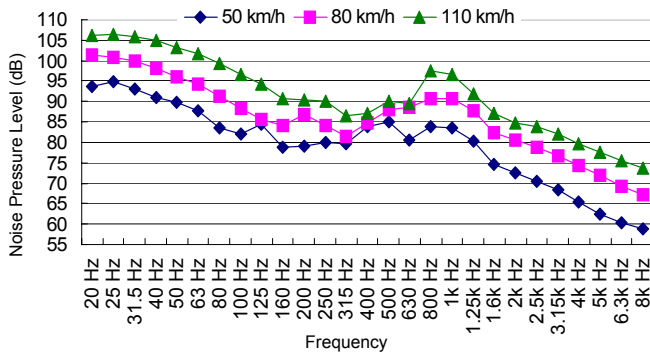


Figure 7. Spectra curves of the noise pressure levels tested from the front inner microphone position under different speeds on arc pavement.

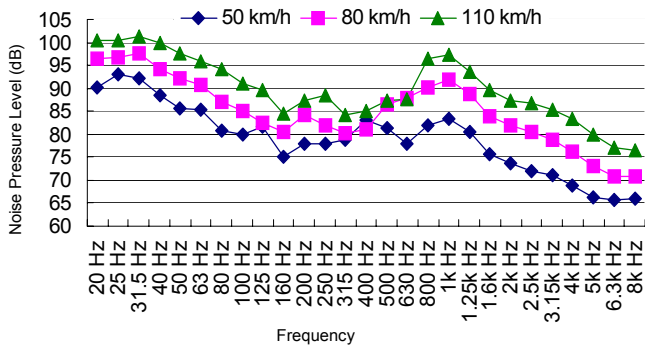


Figure 8. Spectra curves of the noise pressure levels tested from the front inner microphone position under different speeds on ac pavement.

The tread block distance of this tire — LXR (P225/60 97T) is 35 mm. Table 3 shows the results of impact force cha-

racteristic frequencies under the test speeds, calculated with Equation 1. The frequencies of irregular high noise pressure levels measured are also shown in the table. Figures 7 and 8 illustrate the specified irregular high noise pressure levels on the spectral noise level curves corresponding to the ARC and AC pavements.

Table 3. Impact Force Frequency

Speed (km/h)	Impact Frequency Calculated by Equation (Hz)	Frequency of Irregular High Noise Pressure Level (Hz)
50	397	400
80	635	630
110	873	800

Sandberg and Ejsmont (2002) mention that the noise caused by the impact mechanism is the dominant noise source for the related noise frequency range. The noise level of the impact force frequency is about 3 to 5 dB higher than that of adjacent frequencies. This means the sound energy emitted by tread block impact is much higher than that caused by other factors in the related sound frequency band. The Decibel sound level of the center frequency band can be calculated by the following equation (Finch, 2005):

$$L_I = 10 \log_{10} \left(\sum_{i=1}^n 10^{L_{E_i}/10} \right) \tag{2}$$

where L_I represents the noise level of a certain frequency band and L_{E_i} represents the noise level of frequencies of a certain band.

According to the logarithmic equation for the Decibel noise level of a certain frequency band, the highest noise level plays an important role in calculating the noise level of a related sound frequency band. Since the level of impact sourced noise is much higher than adjacent frequencies in the same frequency band, it can be used to represent the noise level of certain frequency bands.

From Table 3, the frequencies of tested irregular high noise pressure levels fit with the calculated impact frequencies very well. Therefore, this proves that irregular noise pressure levels measured are generated by the mechanism of tread impact, which is a major mechanism of structural vibration in tire/pavement noise generation.

5. Numerical Simulation of Tire/Pavement Noise Generated by the Impact Mechanism

It is proven through CPX tests that the impact mechanism is an important mechanism in tire/pavement noise generation especially in terms of the tire rotating within certain frequency ranges. The tire/pavement noise generated by the impact mechanism is also observed in the CPX tests. The wavelength of the impact sourced noise is related to the vehi-

cle's speed and distance between tire block treads. For the sake of a quantitative investigation on the basis of an analytically sound approach, a numerical analysis model based on a FE acoustic-structure coupled method is established to simulate the generated impact noise.

5.1. Finite Element Method Formation

In most engineering practices, the FEM was developed for solving complex elastic structural analysis problems. With the mathematical method becoming rigorous, FEM can be implemented to solve partial differential equations over complex domains such as in structure-fluid coupled problems since the acoustic structure coupled problem can be recognized as a branch of structure-fluid coupled problems. Thus, the FEM can also be applied for solving acoustic structures coupled with the discrete integral of the fluid-structure interaction equation which is written as:

$$\int_{Vol} \frac{1}{c^2} \delta p \frac{\partial^2 p}{\partial t^2} d(Vol) + \int_{Vol} (\{L\}^T \delta p) (\{L\} p) d(Vol) = - \int_S \rho_0 \delta p \{n\}^T \left(\frac{\partial^2}{\partial t^2} \{u\} \right) d(S) \quad (3)$$

where Vol is the volume of the domain, c is sound speed in the propagation medium, δp is a virtual change in pressure ($= \delta p(x, y, z, t)$), t is time, S is the surface where the derivative of the pressure normal to the surface is applied (a natural boundary condition), $\{n\}$ is the unit normal to the interface S , $[L]^T$ matrix operators (gradient and divergence) for three-dimensional coordinates, $\{u\}$ is the displacement vector of the structure at the interface and ρ_0 is the mean air media density.

Equation 3 evolves from the governing acoustic equation. The left hand side of the equation describes the relationship between sound pressure and the coordinate distance and the left hand side describes the acoustic pressure condition on the fluid-structure interface. The parameter S is treated as the interface of the fluid-structure interaction problem.

p in Equation 3 designates the air media pressure and the structural displacement components u_x , u_y and u_z as the dependent variables to be solved. The finite element approximating shape functions for the spatial variation of the pressure and displacement components are given by:

$$p = \{N\}^T \{p_e\} \quad (4)$$

$$u = \{N'\}^T \{u_e\} \quad (5)$$

where $\{N\}$ is the element shape function for the pressure, $\{N'\}$ is the element shape function for the displacements, $\{p_e\}$ is the nodal pressure vector and $\{u_e\}$ represents the nodal displacement component vectors $\{u_{xe}\}$, $\{u_{ye}\}$ and $\{u_{ze}\}$.

Let the matrix operator $\{L\}$ applied to the element shape functions $\{N\}$ be denoted by:

$$\{B\} = \{L\} \{N\}^T \quad (6)$$

Substituting Equation 6 through Equations 5 and 4 into Equation 3, the finite element statement of wave Equation 7 is given by:

$$\frac{1}{c^2} \int_{Vol} \{N\} \{N\}^T d(Vol) \{\ddot{p}_e\} + \int_{Vol} \{B\}^T \{B\} d(Vol) \{p_e\} + \rho_0 \int_S \{N'\} \{n\}^T \{N'\}^T d(S) \{\ddot{u}_e\} = 0 \quad (7)$$

Equation 7 can be written in matrix notation to obtain the discretized wave equation:

$$[M_e^p] \{\ddot{p}_e\} + [K_e^p] \{p_e\} + \rho_0 [R_e] \{\ddot{u}_e\} = 0 \quad (8)$$

where $[M_e^p] = (1/c^2) \int_{Vol} \{N\} \{N\}^T d(Vol)$ is the air media mass matrix, $[K_e^p] = \int_{Vol} \{B\}^T \{B\} d(Vol)$ is the air media stiffness matrix and $\rho_0 [R_e] = \rho_0 \int_S \{N'\} \{n\}^T \{N'\}^T d(S)$ is the coupling mass matrix.

For the tread impact mechanism, the noise is generated by the vibration of the tire tread caused by the interaction between the tire and pavement. For the whole system, the vibration happens not only in the air media domain but also in the structure. Equation 8 can be employed to solve the problem of sound propagation in the air media domain. The excitation is applied on the domain boundary. The equation does not take the structural vibration into account. This problem can be solved by coupling the fluid-structure interaction equation with the structural vibration equation.

The structural vibration equation can be expressed by Equation 9 (ANSYS, 2004):

$$[M_e] \{\ddot{u}\} + [K_e] \{u\} = \{F_e\} \quad (9)$$

where $[M_e]$ is the structural mass matrix, $[K_e]$ is the structural stiffness matrix, $\{\ddot{u}\}$ is the nodal acceleration vector, $\{u\}$ is the nodal displacement vector and $\{F_e\}$ is the applied load vector.

Given that the air media pressure load acts at the acoustic-structural interface, the structural vibration equation is expressed as:

$$[M_e] \{\ddot{u}_e\} + [K_e] \{u_e\} = \{F_e\} + \{F_e^{pp}\} \quad (10)$$

where $\{F_e^{pp}\}$ is the air media pressure load vector at the interface S , which is expressed as:

$$\{F_e^{pp}\} = \int_S \{N'\} \{N\}^T \{n\} d(S) \{P_e\} = [R_e] \{P_e\} \quad (11)$$

Substituting Equation 10 into Equation 11, the dynamic elemental equation of the structure becomes:

$$[M_e]\{\ddot{u}_e\} + [K_e]\{u_e\} - [R_e]\{P_e\} = \{F_e\} \quad (12)$$

By assembling Equations 9 and 12, the finite element discretized equation for the fluid-structure interaction problem is obtained in the form of:

$$\begin{bmatrix} [M_e] & [0] \\ [M^{fs}] & [M_e^p] \end{bmatrix} \begin{Bmatrix} \{\ddot{u}_e\} \\ \{\ddot{p}_e\} \end{Bmatrix} + \begin{bmatrix} [K_e] & [K^{fs}] \\ [0] & [K_e^p] \end{bmatrix} \begin{Bmatrix} \{u_e\} \\ \{p_e\} \end{Bmatrix} = \begin{Bmatrix} \{F_e\} \\ \{o\} \end{Bmatrix} \quad (13)$$

5.2. Model Establishment

5.2.1. Tire/Pavement Acoustic Modeling

The three-dimensional tire/pavement acoustic model established in the research is shown in Figure 9. The model consists of three main subsections—tire, pavement and air media. The tire is established as having the real dimensions of the CPX tire — LXR (P225/60 97T). In the model, the tire contacting with the pavement surface and is covered by air media. The air media is modeled as a sphere because the infinite acoustic element FLUID130, which has the acoustic energy absorption function, can only be effective at the boundary of a body with a spherical shape. The tire structure can be considered symmetric in the axial direction by setting the center of the tire at the origin of the coordinate system. Therefore, it is assumed that the dynamic and acoustic boundary conditions of the tire in the negative and positive axial directions are the same when the tire is rotating on the pavement. To reduce calculation time and save computer resources that are needed for the model calculation, the symmetric relationship is established for the tire/pavement acoustic model. The vertical middle section of the tire is selected as the symmetric surface. The structure of the tire model is shown in Figure 10.

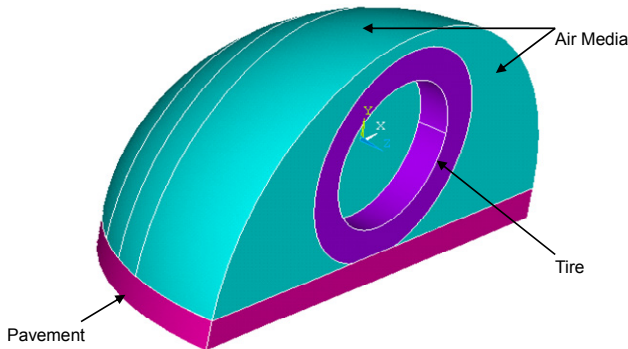


Figure 9. Tire/pavement Acoustic Model.

5.2.2. Element Selection

The 3-D tire/pavement acoustic model is established to evaluate the propagation of the noise generated by the interaction of the tire and pavement. This acoustic model includes seven element types. They are 3-D-fluid elements with and without structure, shell elements, 3-D infinite acoustic elements and 3-D solid element and contact elements. 3-D sound propagation mediums — atmospheric air and the air inside the

tire are meshed with the 3-D-fluid element — FLUID30. The thin thickness parts — tire rubber surface and arm ring are meshed with the shell element -- SHELL63. The solid structure — pavement is meshed with the 3-D solid element — SOLID45 and the outer boundary of the atmospheric air is meshed with the 3-D infinite acoustic element — FLUID130. CONTA173 and CONTA174 elements are employed to simulate the contact relationship between the tire and pavement surfaces. The acoustic model and the meshing of the model are shown in Figure 11.

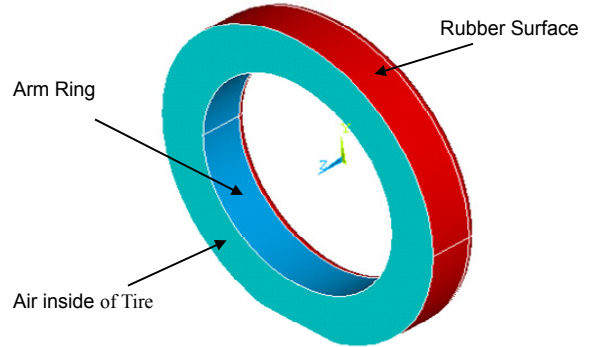


Figure 10. Tire Structure.

The tire is a structure where the air media interfaces both sides of a rubber shell. The energy would be absorbed by the shell material when the sound wave passes across the shell. Therefore, the sound pressures are different on each side of the shell. However, it has been described by some researchers (Maluski and Gibbs, 2000; Nguyen, 2001) that each node in the shell element will have the same pressure on each side of the shell and using shell elements with air media and structure interfaces on both sides will lead to some mistakes.

The double-layer shell method, which is recommended by Howard (2000), is employed to solve this problem. This method is based on the theory that two layers of shells are coincident and the displaced degrees of freedom are coupled but release the freedom of pressure from each layer which is free to correspond with the pressure from each side of the shell. The material properties of the single panel should be adjusted to ensure the material properties of the double layer shell are in accordance with that of a one layer shell. The Young's modulus and density of the double layer shell should be calculated by dividing the modulus of the real material by 2 but the other material prosperities do not need to be changed.

5.2.3. Loads and Boundary Conditions

The sound absorption coefficient indicates how much of the sound is absorbed in the actual material. The absorption coefficient can be expressed as:

$$\alpha = \frac{I_r}{I_i} \quad (14)$$

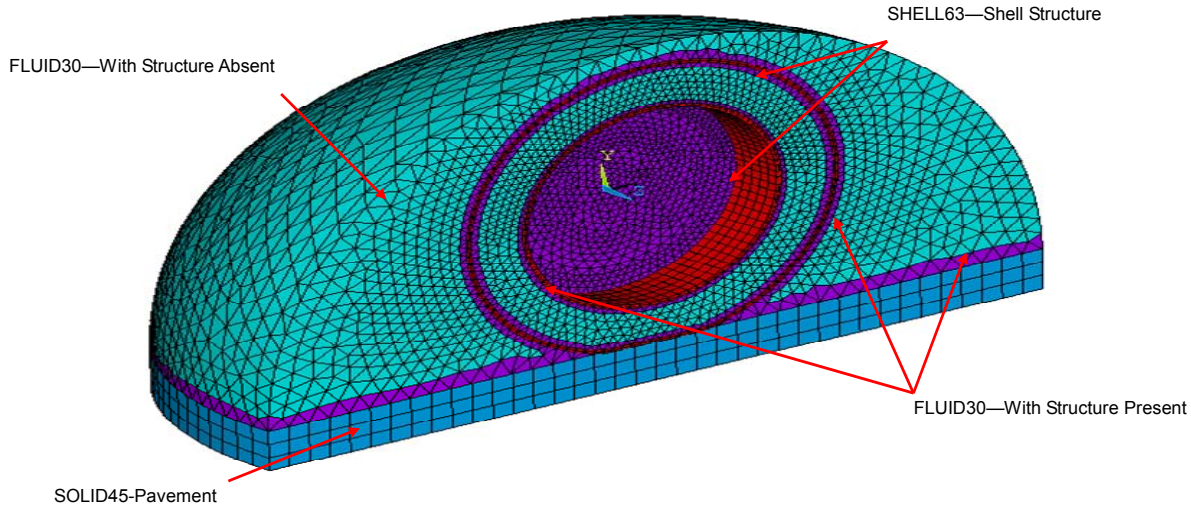


Figure 11. Finite element meshing of tire/pavement noise propagation.

where α is the absorption coefficient, I_r is the reflected sound energy and I_i is the sound energy.

The sound absorption occurs where the two media interact. In the tire/pavement model, there are three material interactions — the air/tire rubber interaction, air/arm ring interaction and tire/pavement interaction. In the previous media, the sound absorption is caused by the sound energy fraction in the media interaction. The sound absorption coefficient can be calculated by the following equation (Kinsler et al., 2000):

$$\alpha(\omega) = \frac{4\rho_i c_i \rho_{ii} c_{ii}}{(\rho_i c_i + \rho_{ii} c_{ii})^2} \quad (15)$$

where ω is the circular frequency, ρ_i and c_i are the density and sound speed of the incidental media and ρ_{ii} and c_{ii} are the density and sound speed of the refracted media.

The sound speed can be calculated by the conventional expression as show in the following equation:

$$c = \sqrt{k/\rho} \quad (16)$$

where k is the bulk modulus and ρ is the density of the media.

However, the pavement is a mixture of different materials. The major materials in AC pavement include sand, gravel, asphalt and on the others. In addition, the ARC pavement is a porous material. There are many voids on the surface and inside the pavement. As a result, the sound absorption area of porous media is largely increased by the voids on the surface and inside the media. Acoustic energy can be absorbed in porous media. Thus, the sound absorption coefficient of porous material is much larger than that of dense material. For the above reasons, in this research, the sound absorption coefficient of pavement is acquired by sound absorption tests rather than theoretical calculations from Equation 15. In refer-

ence to research on sound absorption coefficients of porous and nonporous pavements (Marolf et al., 2004), (Ge and Wang, 2003) and (Zhu and Carlson, 2001), the sound absorption coefficients of the different pavements under the frequencies that should be analyzed are listed in Table 4, where “Conv.” represents the conventional material (AC).

Table 4. Sound Absorption Coefficients (α) of Each Multi-Physics Interface

Air/rubber Interface	Air/Steel Interface	Air/Pavement Interface at 400 Hz		Air/Pavement Interface At 630 Hz	
		ARC	Conv.	ARC	Conv.
0.01	4.2×10^{-5}	0.2	0.1	0.3	0.1

5.2.4. Load Applications

The pressure is applied to the elements, which are located on the treading edge of the tire in the form of harmonic vibration to simulate the impact caused by the road texture. The harmonic frequencies of the applied pressure are decided by Equation 1 to simulate the tread impact phenomenon, which is observed in the CPX tests. In this research, the frequencies 397 and 635 Hz are selected as excitation frequencies to simulate the load condition of the tire at 50 and 80 km/h.

The impact mechanism is caused by the pavement texture hitting the tire tread block while the tire is rotating. In the present research, dynamic movement of the tire is translated into the dynamic load applied to the tire surface. Thus, the tire can be considered unmovable compared with the dynamic loads. All freedoms of the nodes on the arm ring edge are fixed since the spokes connect with the edges of the arm ring and constrain its deformation.

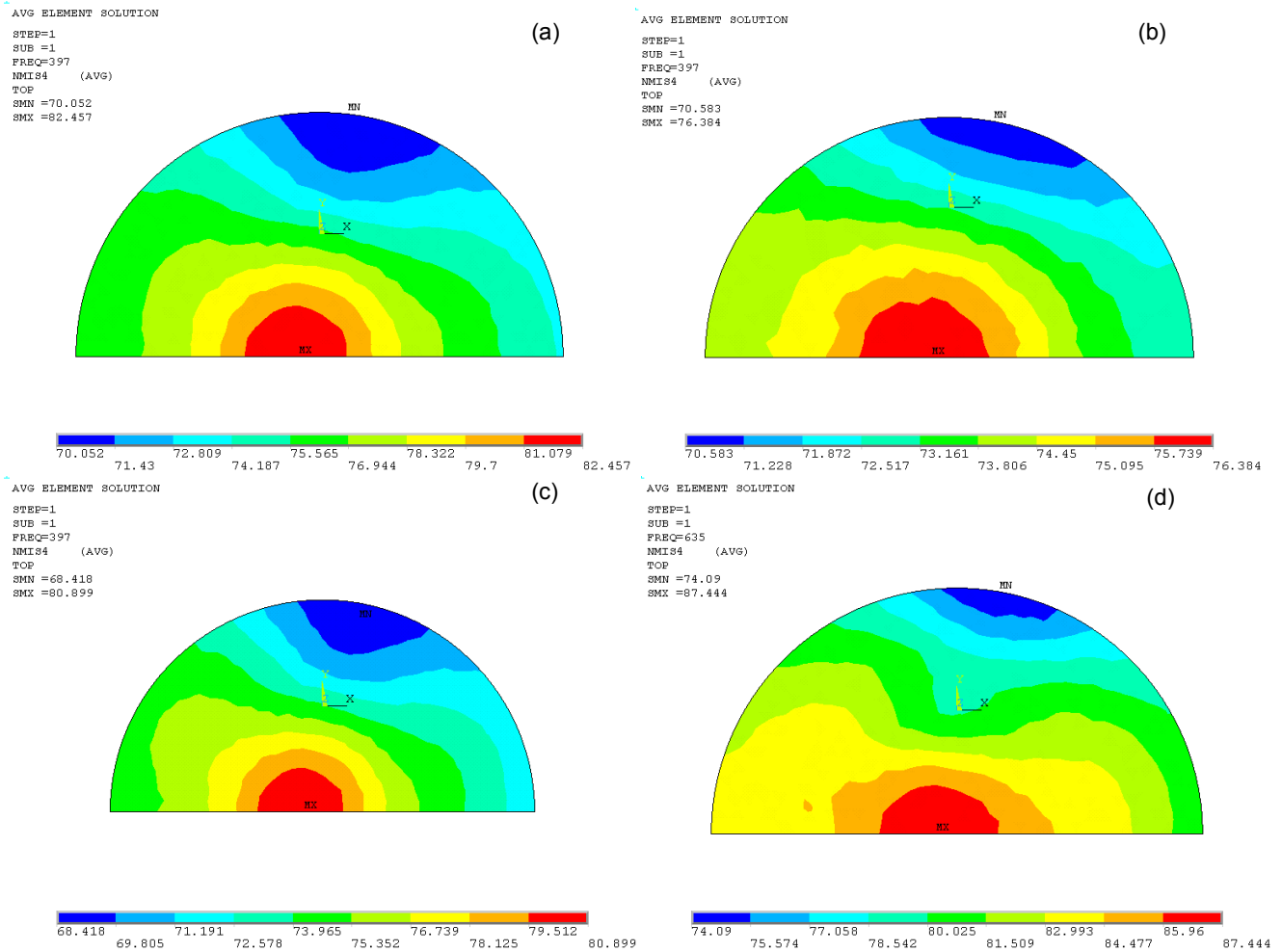


Figure 12. Noise pressure level distributions (in dB) corresponding to the conditions: (a) the inner microphone position under the load pressure frequency 397 Hz and pavement sound absorption coefficient 0.1, (b) outer microphone position under the load pressure frequency 397 Hz and pavement sound absorption coefficient 0.1, (c) inner microphone position under the load pressure frequency 397 Hz and pavement sound absorption coefficient 0.2, (d) inner microphone position under the load pressure frequency 635 Hz and pavement sound absorption coefficient 0.1.

According to the research conducted by Fong (1998), the amplitude of the contact pressure is related to the roughness of the pavement surface and the weight of the vehicle (Fujikawa et al., 2005). The heavier the vehicle, the rougher the pavement responds to the tire. For different degrees of roughness and vehicle weights, the contact pressure ranges from 10^4 Pa to 5×10^5 Pa. Since the highway is a kind of high standard road, the roughness is comparably low compared to other pavements. The trailer is a light vehicle. The contact pressure is comparably low. Thus, in the simulation, 4×10^4 Pa is applied to the treading edge of the tire as the excited load on the AC pavement. The surface of the ARC pavement is much rougher than that of AC pavement. Thus, the tire/pavement impact energy on the ARC pavement should be higher than that on AC pavement. Thus, the excited load on ARC pavement is set at 5.5×10^4 Pa.

5.3. Results and Discussion

Various numerical simulations are performed with the acoustic models established. The noise pressure level distributions are determined for different microphone positions, frequencies and noise absorption coefficients. The noise pressure level distributions are shown in Figure 12. The figures of Figure 12 are the noise pressure level distributions on the cross sections, corresponding to the positions where the microphones are actually located in the field tests.

The noise pressure levels simulated by the FE model are compared with that tested by the CPX test. Figures 13 and 14 show the comparison of tested and simulated noise pressure levels at different microphone positions on the ARC and AC pavements, respectively. From the figures it can be found that the simulated noise pressure levels decrease as the distance increases from the excited source. This agrees with the results

mentioned by Donovan, Oswald (1980) and Ruhala (1999) about tire/pavement noise pressure level distributions tested using NAH and CPI noise mapping techniques.

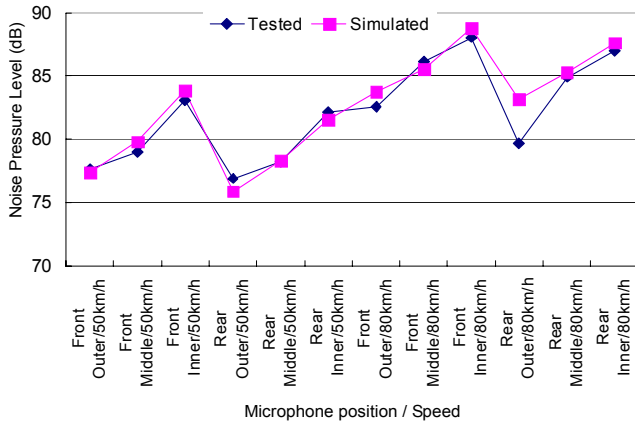


Figure 13. Comparison of tested and simulated noise pressure levels at different microphone positions on conventional pavement.

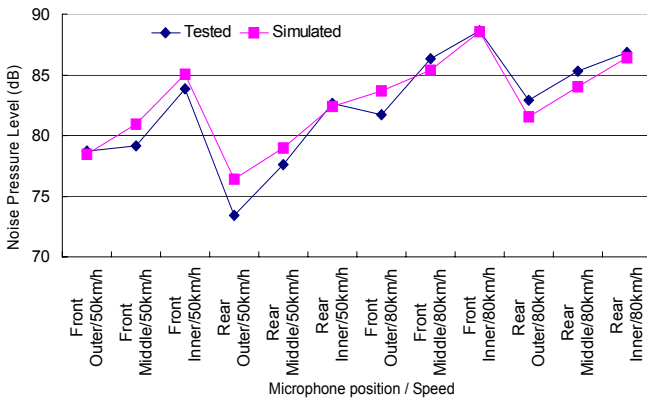


Figure 14. Comparison of tested and simulated noise pressure levels at different microphone positions on arc pavement.

In the comparison between tire/pavement noise levels on ARC and AC pavements, respectively, the paired t-test technique (Goulden, 1956) is used to test the fitness of simulated noise levels and measured noise levels. During the CPX tests, there are six microphone positions for acquisition tire/pavement noise pressures. The two vehicle speeds used for simulation were 50 and 80 km/h. Thus, in total, there are twelve noise pressure levels acquired from the tests. Meanwhile, the tested results are compared with that acquired from the simulation. Paired t-tests adopt a significance level of 0.05. The paired t-test value of the simulated noise pressure with the tested noise pressure levels on ARC pavement is 0.91 and that of AC pavement is 1.37. Both of these t-test values are lower than the t critical value (two-tail) with a sample size of twelve: 1.796. This means the simulated results are acceptable when

compared to the level of significance, 0.05, which implies the simulated results for both ARC and AC pavements fit with the tested results at the 95% confidence level. The numerical models established are there for valid for the acoustic analysis on the propagation of the noise generated by the interactions of the tire and pavements.

6. Concluding Remarks

This research studies tire/pavement noise via experimental and numerical approaches with the comparisons for the noise levels on two different types of pavement — porous pavement (ARC) and nonporous pavement (AC). Close Proximity (CPX) tests are performed in the field to acquire the noise generated from the tire-pavement interaction. A multi-physics finite element (FE) model is established to study the noise generated by the tire/pavement noise with consideration for the impact effects between the tire and pavement surface and the influence of the pavement surface and tire texture structures.

The CPX tests show that for most test options the noise pressure levels on ARC pavement are lower than that on AC pavement. The A-weighted equivalent noise pressure reductions at the rear microphone positions are found to be more significant and the great noise reductions from ARC pavement are found in the tests. The contribution of the aerodynamic sourced noise power absorption of ARC pavement to the noise reduction is evident. From the analysis of the results of spectral noise pressure levels, it is found that the great A-weighted noise reduction at the rear microphone positions can be attributed to the noise pressure reduction in the high frequency range of the spectrum. In terms of the A-weighted equivalent noise pressure levels, the tire/pavement interaction is found to be the major source of tire/pavement noise. Noise frequencies corresponding by the impact mechanism are also identified from the CPX test. The impact mechanism noise frequencies obtained in the field tests compare well with those calculated with the theoretical equation.

Solving the acoustic-structure coupled problem using the structure dynamic method is found very complicated and may cause accuracy concerns. The structural dynamic problem is therefore transferred to a load dynamic problem for the numerical simulation model in this research. The numerical models established consist of the solid, shell and acoustic fluid. The models show reliability, applicability and efficiency in simulating the noise generated by the interaction between a running tire and road surface.

The simulated tire/pavement noise pressure level distributions agree with those of existing studies available in the current literature. Sound absorption considerations are found to play an important role in traffic noise reduction with the ARC material. The results between the tire/pavement noise pressure level simulated using the FE model and that from CPX tests are compared well with implementation of the paired t-test technique. The results generated by the simulation models established can be accepted in 95% confidence level for both the ARC and AC pavements.

References

- Ali, S.A. and Tamura, A. (2003). Road Traffic Noise Levels, Restrictions and Annoyance in Greater Cairo, Egypt, *Applied Acoustics*, 64, 815-823, doi:10.1016/S0003-682X(03)00031-8.
- ANSYS (2004). ANSYS Release 8.1 Documentation Preview.
- de Graaff, D.F. and van Blokland, G.J. (1997). Follow-up Study on the Influence of Metrological Conditions on the Noise of Vehicles during Type Approval, *Report of MVM.95.3.1*, M+P Raadgevende Ingenieurs b.v., 's Hertogenbosch, Netherlands.
- Donavan, P.R., and Oswald, L.J. (1980). The Identification and Quantification of Truck Tire Noise Sources under On-road Operating Conditions, *Research publication GMR-3380*, General Motors Research Laboratories, Warren Michigan, USA.
- Finch, R. (2005). *Introduction to Acoustics*, Pearson Prentice Hall, Upper Saddle River, NJ.
- Fong, S. (1998). Tyre Noise Prediction from Computed Road Surface Texture Induced Contact Pressure, *Proceeding of Inter-Noise*, Christchurch, New Zealand.
- Fujikawa, T., Koike, H., Oshino, Y. and Tachibana, H. (2005). Definition of Road Roughness Parameters for Tire Vibration Noise Control, *Applied Acoustics*, 66, 501-512, doi:10.1016/j.apacoust.2004.08.007.
- Ge, J. and Wang, Z. (2003). The Noise Reduction Analyses of Porous Asphalt Pavement Surface, available at <http://www.sesmag.sh.cn/admin/2/doc/13772.doc>.
- Goulden, C.H. (1956). *Methods of Statistical Analysis*, 2nd ed., John Wiley & Sons, New York.
- Howard, C. (2000). Coupled structural-acoustic analysis using ANSYS, *Internal Report 8th March*, Department of Mechanical Engineering, University of Adelaide.
- IOS (International Organization for Standardization) (1997). Measurement of the Influence of Road Surfaces on Traffic Noise - Part 2, *Close-Proximity Method 11819-2*, Geneva, Switzerland.
- Kinsler, L.E., Frey, A.R., Coppens, A.B. and Sanders, J.V. (2000). *Fundamentals of Acoustics*, 4th ed., John Wiley & Sons, New York.
- Larsson, K., Barrelet, S. and Kropp, W. (2002). The Modelling of the Dynamic Behaviour of Tyre Tread Blocks, *Applied Acoustics*, 63, 659-677, doi:10.1016/S0003-682X(01)00059-7
- Li, B., Tao, S. and Dawson, R.W. (2002). Evaluation and Analysis of Traffic Noise from the Main Urban Roads in Beijing, *Applied Acoustics*, 63, 1137-1142, doi:10.1016/S0003-682X(02)00024-5
- Maluski, S.P.S. and Gibbs, B.M. (2000). Application of a Finite-Element Model to Low-Frequency Sound Insulation in Dwellings, *J Acoust Soc Am.*, 108, 1741-1751, doi:10.1121/1.1310355
- Marolf, A., Neithalath, N., Sell, E., Wegner, K., Weiss, J. and Olek, J. (2004). Influence of Aggregate Size and Gradation on the Acoustic Absorption of Enhanced Porosity Concrete, *Materials Journal*, 101, 82-91.
- Meiarashi, S., Ishida, M., Fujiwara, T., Hasebe, M. and Nakatsuji, T. (1996). Noise Reduction Characteristics of Porous Elastic Road Surfaces, *Applied Acoustics*, 41, 239-250, doi:10.1016/0003-682X(95)00050-J.
- Nguyen, C.H. (2001). Finite-Element Modeling of Low-Frequency Sound Propagation in Test Rooms and Sound Transmission through Partitions, *6th Swiss CAD-FEM Users' Meeting*, Zurich, Switzerland.
- Ruhala, R.J. (1999). A Study of Tire/pavement Interaction Noise Using Nearfield Acoustic Holography, *UMI Miroform 9940945*.
- Sandberg, U. and Ejsmont, J.A. (2002). *Tyre/Road Reference Book*, Informex Ejsmont & Sandberg Handelsbolag, Harg, Sweden.
- World Health Organization (WHO) (1999). Guidelines for Community Noise, Geneva, Switzerland.
- Zhu, H. and Carlson, D. (2001). A Spray Based Crumb Rubber Technology in Highway Noise Reduction Application, *Solid Waste Management*, 27, 27-32.